

# Dust-to-gas Ratio and Metal Abundance in Dwarf Galaxies

U. Lisensfeld<sup>1</sup> & A. Ferrara<sup>2</sup>  
Osservatorio Astrofisico di Arcetri  
Largo E. Fermi 5  
50125 Firenze, Italy

## ABSTRACT

We have compared the metallicity (represented by oxygen abundance),  $X_o$ , and the dust-to-gas ratio,  $\mathcal{D}$ , in a sample of dwarf galaxies. For dwarf irregulars (dIrrs) we find a good correlation between the two quantities, with a power-law index  $0.52 \pm 0.25$ . Blue Compact Dwarf (BCD) galaxies do not show such a good correlation; in addition both the dust-to-gas ratio and the metallicity tend to be higher than for dIrrs. We have then developed a simple but physical analytical model for the above relation. Comparing the model results with the data, we conclude that: (i) for low values of  $\mathcal{D}$ , the  $\mathcal{D} - X_o$  relation is quasi-linear, whereas for higher values the curve strongly deviates from the linear behavior, implying that the commonly used power-law approximation is very poor; (ii) the deviation from the linear behavior depends critically on the parameter  $\chi$ , the “differential” mass outflow rate from the galaxy in units of the star formation rate,  $\psi$ ; (iii) the *shape* of the  $\mathcal{D} - X_o$  curve does not depend on  $\psi$ , but only on  $\chi$ ; however, the specific location of a given galaxy on the curve does depend on  $\psi$ ; (iv) the BCD metallicity segregation is due to a higher  $\psi$ , together with a significant differential mass outflow. Thus, the lack of correlation can be produced by largely different star formation rates and values of  $\chi$  in these objects.

*Subject headings:* ISM: abundances; dust, extinction; galaxies: irregulars; galaxies: evolution  
galaxies: ISM; infrared: galaxies

## 1. Introduction

Interstellar dust consists mainly of heavy elements. Therefore a relation between the dust-to-gas ratio and the metallicity of a galaxy can be expected. The simplest argument to derive this dependence comes from Franco & Cox (1986): the authors suggest that the dust-to-gas ratio,  $\mathcal{D}$ , is simply  $\propto Z$ , the metallicity of the gas. However, this assumption might be too simplistic. Furthermore, the dust-to-gas ratio might be expected to depend on the star formation rate.

Dwek & Scalo (1980) have shown that dust injection from supernovae dominates other sources, if indeed grains can form and survive in the ejecta. This has become clear after the SN1987A event, in which dust has been unambiguously detected (Moseley et al. 1989, Kosaza, Hasegawa & Nomoto 1989). Indeed, the bulk of the refractory elements (characterized by higher melting temperatures, such as Si, Mg, Fe, Ca,

---

<sup>1</sup>Present address: Universidad de Granada, Departamento de Física Teórica y del Cosmos, 18002 Granada, Spain, E-mail: ute@ugr.es

<sup>2</sup>E-mail: ferrara@arcetri.astro.it

Ti, Al etc.) is injected into the ISM by supernovae (McKee 1989). Dust can be destroyed by interstellar shocks: small grains are destroyed by thermal sputtering in fast non-radiative shocks; large grains are destroyed by grain-grain collisions and eroded by non-thermal sputtering in radiative shocks (Jones et al. 1994, Borkowski & Dwek 1995). In addition, dust grains might be expelled from the galaxy either by radiation pressure (Ferrara et al. 1991) or convected away by a fountain-like flow (Norman & Ikeuchi 1989). From these arguments, it follows that the dust content of a galaxy is clearly governed by supernovae, and therefore the equilibrium established between the formation and destruction processes could be influenced by the star formation history of the galaxy.

The aim of this paper is to investigate these processes. As a first step we want to ascertain empirically the existence of a relation between the dust-to-gas ratio, metallicity and the star formation activity. The results are used to constrain a model for the dust production taking into account the processes described above. We have selected dwarf galaxies as objects for this study. The reason is twofold: (i) the metallicities observed in these objects span a large range of values; (ii) due to their small size and simple structure, radial gradients in the dust-to-gas ratio and metallicity can be neglected. Both features make them suitable objects for a comparison of the dust-to-gas ratio and metallicity. The knowledge of the dust content in dwarf galaxies is also relevant to cosmological studies as dwarfs represent the most numerous population of galaxies. Thus, their dust content could have important implications, e.g. for the obscuration of QSOs.

Detailed studies of the extinction properties of the Magellanic Clouds have revealed a clear relation between the dust-to-gas ratio and the metal abundance: In the Large Magellanic Cloud (LMC) both the metallicity and the dust-to-gas ratio are roughly a factor 4 lower than in the Galaxy (Koornneef 1982; Fitzpatrick 1986) and in the Small Magellanic Cloud (SMC), where the metallicity is a factor of about 10 lower than in the Galaxy, also the dust-to-gas ratio is a factor of 8 - 11 lower (Bouchet et al. 1985). So far only few studies have investigated the relation between the dust-to-gas ratio and the metallicity for a large number of galaxies. Issa, MacLaren & Wolfendale (1990) have compared the dust-to-gas ratio and the metallicities in the Galaxy and 6 nearby galaxies and found evidence for a correlation, with the two quantities decreasing at roughly the same rate with increasing galactocentric radius. When taking both quantities at a fixed radius they also obtained a good correlation, following  $Z \sim \mathcal{D}^{0.85 \pm 0.1}$ . Schmidt & Boller (1993) have compared the dust-to-gas ratio and metallicity of 23 nearby dwarf galaxies and found that the oxygen abundance is  $\sim \mathcal{D}^{0.63 \pm 0.25}$ , hence in good agreement with Issa et al. (1990).

In the present work we have compiled data for dwarf irregular (dIrr) galaxies and blue compact dwarf (BCD) galaxies from the literature and studied the relation between the dust and metal abundance and the star formation rate. For the dIrr sample we confirm the existence of a correlation which is clearly non-linear whereas for the BCD sample no significant correlation could be found. These results allow a theoretical insight on the physics that governs the metal and dust production and on global galactic properties such as the star formation and mass loss history.

## 2. The samples and the data

We divide the dwarf galaxies in our study into two subsamples: one sample contains dIrr galaxies and the other sample consists of BCDs. In the dIrr sample we include all galaxies of morphological type S(B)m or I(B)m without applying a, in any case arbitrary, luminosity cutoff. The reason for distinguishing between dIrrs and BCDs is their different recent star formation history: BCDs possess spectra very similar to H II regions, and they are believed to be undergoing a starburst. This variable, intense star formation rate in

the recent past could affect the relation between the dust and metal abundance, as the time scale for a starburst ( $\approx 10^7 - 10^8$  years) is comparable to the time scales relevant for the dust and metal production which is given by the life time of massive stars. Most of the dIrrs, on the other hand, are not in such an extremely intense star forming phase.

In Tab. 1 and 2 the data for the samples are listed. The sample of dIrrs consists of 28 galaxies. The sample size was mainly constrained by the availability of metallicity data. The oxygen abundances, which were chosen as a tracer for the metallicity, were taken from a compilation of Skillman, Kennicutt & Hodge (1989), Hunter, Gallagher & Rautenkranz (1982) (corrected according to McGaugh 1991), Campbell, Terlevich & Melnick (1986) and Schmidt & Boller (1993). The latter authors did a similar study to the present one; their sample contains 23 dIrr galaxies and is a subsample of ours. The rest of the data (far-infrared (FIR) flux, distance, blue luminosity, H I mass, optical diameter) were taken from the catalogue of Melisse & Israel (1994a) except for NGC 4236 which was not included in their sample. For this galaxy we took the blue magnitude from de Vaucouleurs et al. (1991) (Third Reference Catalogue, RC3) and the H I flux from Huchtmeier & Richter (1989).

The BCD sample contains 16 galaxies. We have restricted the sample to small galaxies (optical diameter less than 10 kpc) in order to obtain a sample of galaxies comparable in size to the dIrrs. The metallicities and distances were taken from Kunth & Sèvre (1986), Masegosa, Moles & Campos-Aguilar (1994) and Terlevich et al. (1992). The H I fluxes are from the Huchtmeier & Richter (1989), Huchtmeier, Hopp & Kuhn (1997), Stavely-Smith, Davies & Kinman (1992) and from RC3. The FIR fluxes were taken from the IRAS Faint Source Catalogue (1990).

The H I mass is derived from the H I flux,  $S_{HI}$  as:

$$M_{HI} = 2.36 \cdot 10^5 \left( \frac{S_{HI}}{\text{Jy km s}^{-1}} \right) \left( \frac{D}{\text{Mpc}} \right)^2 M_{\odot}. \quad (1)$$

### 2.1. Calculation of the dust mass

The dust masses were calculated from the FIR emission using a single temperature, black-body model:

$$M_{\text{dust}} = \frac{f_{100} D^2}{B(\nu, T_{\text{dust}}) Q_{\nu}} \quad (2)$$

where  $B(\nu, T_{\text{dust}})$  is the Planck emission function,  $D$  the distance to the galaxy,  $f_{100}$  the IRAS flux at  $100\mu\text{m}$  and  $T_{\text{dust}}$  the dust temperature. The infrared dust absorption coefficient,  $Q_{\nu}$ , is assumed to be the same for all galaxies and was taken from Hildebrand (1983):

$$Q_{\nu} = 0.1 \left( \frac{250}{\lambda} \right)^{\beta} \text{ g/cm}^2; \quad (3)$$

$T_{\text{dust}}$  is calculated from the ratio of the IRAS fluxes at 60 and 100  $\mu\text{m}$ . Together this yields:

$$M_{\text{dust}} = 12 \left( \frac{f_{100}}{\text{Jy}} \right) \left( \frac{D}{\text{Mpc}} \right)^2 \left( \frac{250}{100} \right)^{-\beta} \left\{ \left[ \frac{f_{100}}{f_{60}} \left( \frac{100}{60} \right)^{\beta+3} \right]^{1.5} - 1 \right\} M_{\odot} \quad (4)$$

We assumed  $\beta = 2$ . The choice of  $\beta$  has only a minor influence on the dust mass.

## 2.2. Uncertainties in the dust mass calculation

The dust mass inferred from the FIR emission as described above is affected essentially by two main uncertainties.

First, the value of the dust mass calculated as described above depends sensitively on the dust temperature derived from the 60-to-100 $\mu\text{m}$  flux ratio. We assume hereby that both the 60 and the 100 $\mu\text{m}$  flux is dominated by the emission of big grains, that contain most of the dust mass, and are in thermal equilibrium with the radiation field. If very small grains (VSGs), whose temperature is fluctuating, contribute significantly to the 60 $\mu\text{m}$  emission this method produces wrong results. An analysis of the Galactic diffuse, 'cirrus', emission and extinction curve in the solar neighborhood (Désert, Boulanger & Puget 1990) has shown that the emission of VSGs could indeed be responsible for 60% of the 60 $\mu\text{m}$  flux, but only for 15% of the flux at 100 $\mu\text{m}$ . Since the contribution of VSGs to the dust mass is negligible, this results in an error in the dust mass of a factor 3. A similar result was obtained by Sodrowski et al. (1987) who analyzed the FIR emission in our Galaxy and found that the dust temperature derived from the 60/100 $\mu\text{m}$  ratio stays almost constant with Galactic radius in spite of the decreasing radiation field. A possible interpretation is that the 60 $\mu\text{m}$  emission is to a large extent produced by VSGs. The apparent dust-to-gas mass ratio derived from the FIR emission with this constant temperature profile decreased by a factor of 3 outwardly. Assuming that the dust-gas ratio is the same everywhere in the Galaxy, the implied error of the dust mass in this analysis is also a factor of 3.

However, the contribution of VSGs to the 60 $\mu\text{m}$  flux is expected to be only significant in a low radiation field in which the big grains have a low temperature and contribute little to the 60 $\mu\text{m}$  emission (Désert et al. 1990). This is not the case for dwarf galaxies which show higher 60/100 $\mu\text{m}$  and lower 12/25 $\mu\text{m}$  ratios than spiral galaxies (Xu & de Zotti 1991, Melisse & Israel 1994b) indicating a lack of 'cirrus' emission. Therefore we can expect that the error due to VSGs is smaller than estimated for the Galactic cirrus emission. We have carried out the following qualitative test for this assumption: If the dust temperature derived from the 60 and 100 $\mu\text{m}$  fluxes is a good measure for the real temperature of the big grains, it should correlate with the radiation field. In Fig. 1 the dust temperature and the surface brightness of the bolometric luminosity for both samples are plotted. The bolometric luminosity was calculated as described below and the galaxy surface area is obtained from the optical diameter. A good correlation between the dust temperature and the bolometric surface brightness is visible. The correlation coefficient (only detections) is  $r = 0.75$ . This supports our assumption that the dust temperature represents the temperature of big grains in thermal equilibrium.

Next, the dust-to-gas ratio derived from the FIR emission is generally significantly, up to a factor of 10, lower than the value found from the analysis of the extinction in the Solar Neighborhood. This has been found both for simple blackbody models like the present one (Young et al. 1989; Devereux & Young 1990) as well as for more detailed dust models (Rowan-Robinson 1992). The presence of cold dust, emitting mainly beyond 100  $\mu\text{m}$ , might be responsible for the discrepancy. On the basis of the available data it is not possible to decide about this point, observations at longer wavelengths would be necessary. Because of this uncertainty we have carried out a further test to check whether our dust masses are reasonable: We have compared them with an alternative way to estimate the dust mass, through an energy balance between the fraction of the radiation absorbed by the dust and escaping from a galaxy (Xu & Buat 1995; Xu & Helou 1996). From the fraction of nonionizing radiation absorbed by the dust we can estimate the dust opacity and from that, assuming that the opacity produced by a certain dust mass is the same as in the Galaxy, the dust mass per area can be calculated. We have calculated the fraction of radiation absorbed by dust

following the model of Xu & Buat (1995) who estimate the bolometric luminosity from the ultraviolet ( $f_{UV}$ ), blue ( $f_B$ ) and FIR fluxes. For our sample, the ultraviolet (UV) fluxes were available for only 9 galaxies (taken from Fanelli et al. 1997; Hill et al. 1994; Deharveng et al. 1994; Donas et al. 1987; Donas & Deharveng 1984). For these we derived  $f_B/f_{2000\text{\AA}} = 1.0$  which we use for the whole sample.

The ratio of the FIR-to-bolometric luminosity gives the fraction of radiation absorbed by the dust. If our dust mass estimate is correct, this value should be related to the dust mass per surface area. Indeed, we found a good correlation between these two quantities ( $r = 0.87$ ). In order to quantify this further we have to make a distinction between dust emission from H II regions and diffuse dust emission. The dust in H II regions is mainly heated by ionizing photons which are almost completely absorbed by the dust locally, practically independent of the dust amount. The diffuse dust, on the other hand, is mainly heated by nonionizing photons and the amount of radiation absorbed is directly related to the dust opacity. Thus, in order to calculate the (diffuse) dust opacity we have to subtract the dust heating by ionizing photons. We estimate the ionizing UV radiation from the  $H_\alpha$  emission. The total  $H_\alpha$  fluxes were available for a large part of the dIrr sample (18 galaxies,  $H_\alpha$  fluxes taken from Hunter, Hawley & Gallagher 1993, Hunter et al. 1989, Kennicutt & Kent 1983). Since the dust opacity is generally low in dwarf galaxies, the extinction of the  $H_\alpha$  line is likely to be small and we neglected it. The total dust emission originating from ionizing radiation can be estimated as  $f_{\text{dust}}^{\text{lyc}} = 27.12 \times f_{H_\alpha}$  (Xu & Buat 1995). The average fraction of dust emission due to heating by ionizing photons is  $f_{\text{dust}}^{\text{lyc}}/f_{\text{dust}} = 0.45 \pm 0.35$ , where  $f_{\text{dust}}$  is the total dust emission, extrapolated from the FIR emission according to Xu & Buat (1995). We use this average value for the galaxies for which no  $H_\alpha$  data is available.

The diffuse dust opacity is estimated using a simplified radiation transfer model with a slab geometry, assuming that dust and stars are homogeneously mixed. In view of the uncertainty of the real diffuse dust distribution in the individual galaxies this simplification seems to be justified. A different geometry, e.g. a ‘sandwich distribution’ or a clumpy dust distribution would lead to a different value for the dust opacity and the dust mass. A crucial assumption in the present test is therefore that there is no *systematic* change in the diffuse dust morphology, i.e. that there is no correlation between the geometry (e.g. clumpiness) and the absorbed fraction of radiation, dust-to-gas ratio or metallicity. We use an approximate formula (Xu & de Zotti 1989) for the dust absorption probability, further simplified by dividing the nonionizing radiation into two (optical and UV) bands for which we take the extinction properties at 4300 Å and 2000 Å, respectively (see Lisenfeld, Völk & Xu 1996).

The opacities deduced (at 4300 Å),  $\tau_B$ , range between 0.01 and 0.4. Assuming that the dust has the same extinction properties as dust in our Galaxy (Désert et al. 1990), we can estimate the dust mass as

$$M_{\text{dust}}^{\text{opa}} [M_\odot] = 8.8 \cdot 10^4 \times \tau_B \times \left( \frac{A_{\text{gal}}}{\text{kpc}^2} \right) \quad (5)$$

where  $A_{\text{gal}}$  is the optical surface area of the galaxy. In Fig. 2 the dust mass estimated in this way and the dust mass calculated from the FIR emission are compared. The most striking result is the very good ( $r = 0.96$ ) and linear (slope =  $1.0 \pm 0.05$ ) correlation between the two quantities. The dispersion around the regression line is 0.34 dex, corresponding to a factor of 2.2. The dust mass derived from the FIR emission is on average a factor of 29 lower than the mass derived from the opacity. However, since the main aim of the present work is the comparison of the dust-to-gas ratio with the metallicity of galaxies, the absolute value of the dust mass is only of secondary importance; the crucial point is that the *ratio* of the dust masses is correct. The linear correlation between the dust masses derived in two different ways (from the FIR emission and from the extinction) corroborates that this latter assumption is correct.

### 3. Comparison of the dust-to-gas ratio and the metallicity

In Fig. 3 - 5 the dust-to-gas ratios and the metallicities are plotted for the two samples. For the galaxies with upper limits in both IRAS fluxes, the dust temperature is undefined and therefore, strictly speaking, the dust mass as well. Since the dust temperature in the samples shows a small dispersion (all values lie between 22 and 42 K) we adopted  $T = 30$  K for these 4 dIrr galaxies and calculate the dust mass with this value in order to give at least an indicative value (filled squares in in Fig. 3 - 5). In the same way, we adopt for the BCDs that were not detected by IRAS an upper limit of 1 Jy at 100  $\mu\text{m}$  and a dust temperature of 32 K, corresponding to the average value found for this sample.

We only considered the H I gas mass in our analysis. The extent of the H I emission is generally much larger than the optical diameter. Fouqué (1983) has found that on average for irregular galaxies the H I effective radius (i.e. the radius within which half of the H I gas is contained),  $D_{HI}$ , and the optical isophotal radius,  $D_{25}$ , are nearly the same,  $\log(D_{HI}/D_{25}) = 0.04 \pm 0.2$ . Even if there is dust associated with this extended H I it is, due to the absence of heating sources, very cold and therefore unlikely to contribute to the FIR emission. Therefore, in order to get an accurate value for the dust-to-gas ratio within the optical disk, we only consider the H I mass within the optical disk,  $M_{HI,opt}$ , by dividing the total H I mass by 2.

We could not derive H<sub>2</sub> masses for the whole sample because of the lack of data. We expect the error to be small, at least for dwarf irregulars, since the molecular gas content is generally much less than the atomic gas content: Whereas the molecular mass content of spiral galaxies is in general roughly comparable to the atomic gas content with a median value of  $M(\text{H}_2)/M(\text{H I}) = 0.5$  (Andreani, Casoli & Gerin 1993; Devereux & Young 1990), in dwarf irregular this ratio is lower. Cohen et al. (1988) derived in the LMC a molecular-to-atomic gas fraction of 30%. Molecular hydrogen absorption measurements gave an even lower value of 6 % (Clayton et al. 1996). For the SMC the molecular-to-atomic gas ratio is estimated to be 7% (Rubio et al. 1991). For 7 galaxies of our sample we could find CO data in the literature (Young et al. 1995, Elfhag et al. 1996). The conversion factor from H<sub>2</sub> to CO is extremely uncertain for dwarf galaxies and very likely to be considerably higher than the standard value used for Galactic molecular gas clouds. The conversion factors found for the Magellanic Clouds are 6 times higher than for the Galaxy (LMC, Cohen et al. 1988) and 20 times higher (SMC, Rubio et al. 1991). Adopting an intermediate value of 10 times the Galactic conversion factor we obtained only for one Galaxy (NGC 6764) a molecular gas mass larger than the atomic gas mass. It is difficult to assess the possible error caused by neglecting molecular gas, however the above considerations have shown that the likely error caused is less than a factor of 2.

We estimate the total error in the dust-to-gas ratio derived in this way to be about a factor of 4. This number takes into account the possible error in the dust mass due to VSGs (factor 2), cold dust (factor 2, estimated from the dispersion of the correlation in Fig. 2), molecular gas (factor 2), and a varying H I /optical diameter (factor 1.6).

For the dIrr sample there exists a good correlation between the dust-to-gas ratio and the metallicity (Fig. 3). Only one galaxy (GR8) is clearly off the correlation. Not taking into account this galaxy and the 4 galaxies with only upper limits in the FIR, the correlation coefficient is  $r = 0.83$ . The correlation is not linear; a least square fit yields:  $12 + \log(\text{O}/\text{H}) \propto (0.52 \pm 0.25) \times \log(M_{\text{dust}}/M_{\text{HI}})$ . The error in the slope takes into account the dispersion of the data points around the least-square fit line, the error in the dust mass of a factor 4 and an error in the metal abundance of 0.2 dex. This result is in agreement with earlier studies: Schmidt & Boller (1993) obtained a very similar slope in the correlation as we ( $0.63 \pm 0.25$ ) which is to be expected because our sample is an extension (7 more galaxies) of theirs. The results of Issa et al. (1990) who compared the dust-to-gas ratio in nearby galaxies are similar. From their data a slope of

$0.85 \pm 0.1$  can be obtained (Schmidt & Boller 1993).

The sample of the BCDs shows no obvious correlation between the dust-to-gas ratio and the metallicity (Fig. 4). Both the average dust-to gas ratio as well as the average metallicity tend to be higher for this sample than for the dIrrs (Fig. 5). For a given metallicity the dust-to-gas ratio is on average higher than for the dIrr galaxies.

## 4. Model

We are now interested in developing a simple model that explains the observed behavior of the dust-to-gas/metallicity relation in dwarf galaxies. In particular one would like to understand (i) the physics that governs the observed relationship (ii) the apparently different trend found in dIrrs and BCDs (iii) learn about star formation, metal production, and mass loss history of these objects.

### 4.1. Basic Equations

To answer the above questions, we start writing the equations describing the rate of change of the galactic gas mass,  $M_g$ , the mass fraction of a given heavy element  $i$ , denoted by  $X_i = M_i/M_g$  ( $M_i$  is the mass of the element  $i$ ), and the ratio between the mass in element  $i$  and the dust mass,  $f = M_d/M_i = M_d/X_iM_g$ :

$$\frac{d}{dt}M_g = -\psi + E - W, \quad (6)$$

$$\frac{d}{dt}M_i = \frac{d}{dt}[X_iM_g] = -X_i\psi + E_i - X_iW, \quad (7)$$

$$\frac{d}{dt}M_d = \frac{d}{dt}[fX_iM_g] = -\alpha fX_i\psi + f_{in}E_i - \frac{fX_iM_g}{t_{sn}} - \delta fX_iW. \quad (8)$$

We now discuss in detail the various quantities entering eqs. 6-8. The star formation rate (SFR) is denoted by  $\psi$ ;  $E$  is the total injection rate from stars of all masses and ages;  $E_i$  is the total injection rate of element  $i$  from stars;  $W$  is the net outflow rate from the galaxy. The three parameters in eq. 8  $\alpha$ ,  $f_{in}$  and  $\delta$  refer to dust properties:  $\alpha f$  is the fraction of dust destroyed during star formation ( $\alpha = 1$  corresponds to destruction of only the dust incorporated into the star,  $\alpha > 1$  [ $\alpha < 1$ ] corresponds to a net destruction [formation] in the protostellar environment);  $f_{in}$  is the value of the dust fraction in the injected material;  $\delta$  accounts for a possible different dust content of the outflow with respect to the general interstellar medium ( $\delta = 0 \Rightarrow$  no dust in the outflow;  $\delta = 1 \Rightarrow$  the outflow is as dusty as the ISM). It is easy to understand the physical meaning of the above equations from an inspection of the various terms. Eq. 6 and 7 describe the detailed balance of the gas and  $i$ -element mass as due to star formation, stellar injection and outflows; eq. 8 accounts for the fact that dust is destroyed/formed during star formation processes, it is injected by stellar sources, destroyed by supernova shocks (on a characteristic time-scale  $t_{sn}$ ) and lost in outflows. We have neglected the change of  $M_i$  deriving from grain destruction in comparison with the stellar metal production; this approximation holds for values  $\mathcal{D} \lesssim 10^{-3}$  and therefore should be appropriate for our sample; also eq. 8 does not take into account the possible formation or accretion of dust directly in the interstellar medium. The validity of this assumption is difficult to assess, since the determination of the grain accretion rate in the ISM would require a detailed knowledge of the grain microphysics. However, since accretion is well

known to occur preferentially in high gas density regions (molecular clouds), we hope that this process, due to the paucity of molecular gas in dwarfs galaxies, will not have a dramatic impact on our results.

We next adopt the *Instantaneous Recycling Approximation*, (IRA) i.e. stars less massive than  $1 M_\odot$  live forever and the others die instantaneously, (Tinsley 1980) which allows  $E$  and  $E_i$  to be written respectively as

$$E = R\psi; \quad E_i = [RX_i + y(1 - R)]\psi, \quad (9)$$

(Note that Tinsley’s eq. 3.14 contains a wrong extra factor  $1 - X_i$ , see Maeder 1992), where  $R$  and  $y$  are the standard returned fraction (the fraction of the total mass that has formed stars which is subsequently going to be ejected into the ISM) and net stellar yield (the total mass of an element  $i$  ejected by all stars back into the ISM per unit mass of matter locked into stars), respectively. The limitations of IRA are discussed by Tinsley (1980). Some contribution to the dust mass can come from evolved stars, whose evolution is only roughly described by the IRA approximation. However, since we will show below that the major constituent of grains is oxygen – almost totally contributed by massive stars, we estimate that IRA should suffice for our purposes, even though the complete validity of this assumption should be assessed by future studies. Moreover, we assume that the outflow rate is  $W = w\psi$ , with  $w = \text{const.}$ , a common *ansatz* in chemical evolution models. It is also useful for our purpose to write the above equations in terms of the dust-to-gas ratio,  $\mathcal{D} = f X_i$ . With these positions, eqs. 6-8 become

$$\frac{1}{\psi} \frac{d}{dt} M_g = (R - 1 - w) \quad (10)$$

$$\frac{M_g}{\psi} \frac{d}{dt} X_i = y(1 - R) \quad (11)$$

$$\frac{M_g}{\psi} \frac{d}{dt} \mathcal{D} = -[R - 1 - w(1 - \delta) + \alpha] \mathcal{D} + f_{in}[RX_i + y(1 - R)] - \frac{M_g}{t_{sn}} \frac{\mathcal{D}}{\psi} \quad (12)$$

To determine  $t_{sn}$  we follow McKee (1989), who writes this quantity as

$$t_{sn} = \frac{M_g \gamma^{-1}}{\bar{\epsilon} M_s(100)} \quad (13)$$

where  $\gamma$  is an “effective” supernova rate calculated including both Type II and Type I supernovae and accounting for the fact that not all the SNRs interact with the galactic ISM. For sake of simplicity, and also because the second effect should be less important in small objects like dwarf galaxies, we neglect these complications and take  $\gamma$  as the Type II SN rate. We write  $\gamma = \nu\psi$ , where  $\nu$  is the number of supernovae per unit stellar mass formed. We assume  $\nu$  to be the same as in the Galaxy, for which  $\psi \sim 3M_\odot \text{ yr}^{-1}$  (Larson 1996) and  $\gamma \sim 0.022 \text{ yr}^{-1}$  (van den Bergh 1983); this yields  $\nu = 1/136M_\odot = 3.610^{-36} \text{ g}^{-1}$ . The mean efficiency of grain destruction by a shock is denoted by  $\bar{\epsilon}$ ; its precise value depends on the mean gas density and magnetic field strength in the ambient medium. Lacking a precise determination of these quantities in dwarf galaxies, we adopt the conservative value  $\bar{\epsilon} = 0.1$ , suggested by McKee (1989) for the Galaxy. Next we need an estimate for  $M_s(100)$ , the gas mass shocked to a velocity of at least  $100 \text{ km s}^{-1}$ . From the Sedov-Taylor solution in an homogeneous medium one can easily obtain:

$$M_s(100) = 6800 \left( \frac{E}{10^{51}} \right) \left( \frac{v_s}{100 \text{ km s}^{-1}} \right)^{-2} M_\odot \quad (14)$$



where  $E$  is the energy release by the explosion and  $v_s$  is the shock velocity. We adopt the fiducial value  $100 \text{ km s}^{-1}$  in eq. 14 according to McKee (1989). In conclusion, we have

$$t_{sn} = \frac{M_g}{\beta\psi} \quad (15)$$

with  $\beta = \bar{\epsilon}\nu M_s(100) \sim 5$ .

Since we are interested in the relation between  $X_i$  and  $\mathcal{D}$  in order to compare it with the data, we eliminate time from the previous equations. This yields

$$\frac{d\mathcal{D}}{dX_i} + a\mathcal{D} - bX_i = c, \quad (16)$$

where

$$a = \frac{[R - 1 - w(1 - \delta) + \alpha + \beta]}{y(1 - R)}, \quad b = \frac{f_{in}R}{y(1 - R)}, \quad c = f_{in}. \quad (17)$$

The solution of eq. 16 is

$$\mathcal{D}(X_i) = \frac{b}{a}X_i + (1 - e^{-aX_i})\left(\frac{c}{a} - \frac{b}{a^2}\right) \quad (18)$$

In order to quantify the above relation, we need to fix the value of  $R$  and  $y$  for the traced heavy element. We choose oxygen for the following reasons: (i) it is produced mainly in Type II SNe, which are also the ones responsible for the grain shock destruction; (ii) oxygen is the main constituent of grains (the relative abundances of atoms of O:C:Si:Mg in grains are 100:54:6.5:5.2); (iii) a large sample of dwarf galaxies with good quality abundance data for this species is available (see Sect. 2). We therefore take  $X_i \equiv X_o$ , the oxygen mass fraction. The returned fraction and the net yield can be obtained using the standard formulae (Maeder 1992):

$$R = \frac{\int_{m_l}^{m_u} (m - w_m)\phi(m)dm}{\int_{m_l}^{m_u} m\phi(m)dm}; \quad y = \frac{1}{(1 - R)} \frac{\int_{m_l}^{m_u} mp_m\phi(m)dm}{\int_{m_l}^{m_u} m\phi(m)dm} \quad (19)$$

where  $\phi(m)$  is the initial mass function (IMF) defined between the lower and upper masses  $m_l = 1M_\odot$  and  $m_u = 120M_\odot$ , and  $w_m$  ( $w_m = 0.7M_\odot$  for  $m \leq 4M_\odot$  and  $w_m = 1.4M_\odot$  for  $m > 4M_\odot$ ) is the remnant mass (white dwarf or neutron star). We have used a power law form of the IMF,  $m\phi(m) \propto m^{-x}$  with  $x = 1.35$  (standard Salpeter) and  $x = 1.7$  (Scalo 1986). We have taken the oxygen stellar yield,  $p_m$  (i.e. the mass fraction of a star of mass  $m$  converted into oxygen and ejected) from Arnett (1990). With these assumptions we obtain  $R = (0.79, 0.684)$  and  $y = (0.0871, 0.0305)$  for the (Salpeter, Scalo) IMF, respectively.

As a consistency check of our simple chemical and dust evolution model one could try to reproduce, at least qualitatively, the observed  $(12 + \log(O/H) - \log \mu)$  relation, where  $\mu = M_g/M_*$  is the ratio between the gas and stellar mass of the system. From eqs.10-11, it is easy to obtain that

$$X_o = \frac{y(1 - R)}{(1 - R - w)} \ln \left[ \frac{1 + \mu + (w/(1 - R))}{\mu} \right]. \quad (20)$$

The experimental determination of  $\mu$  is very uncertain because it is difficult to derive reliable values for  $M_*$ . However, we have been able to reasonably constrain the value of  $\mu$  for seven dIrrs in our sample from their H-band ( $1.6 \mu\text{m}$ ) luminosity and we find  $0.05 < \mu < 2$ . Using  $w \sim 20 - 40$ , the above formula reproduces quite satisfactorily the observed trend and numerical value of the metallicity-abundance relation. This outflow rate, as we show in the next Section, is very close to the one we require to explain the dust-to-gas ratio of dwarf galaxies.

## 4.2. Model Results

Once  $R$  and  $y$  have been fixed, the solution given by eq. 18 contains four free parameters:  $\alpha, f_{in}, w, \delta$ . However, the solution is quite insensitive to  $\alpha$ : we take it equal to unity. Thus, we are left with three free parameters. The precise value of  $f_{in}$ , the dust-to-O mass ratio in stellar dust sources, is rather uncertain; a simple estimate can be obtained as follows. A typical SN ejects  $\sim 4M_{\odot}$  of heavy elements into the ISM. However, only the fraction of oxygen (which dominates the ejected material) that can bind to refractory elements can go into grains, at most 25% as derived from ISM depletion studies. In addition a rather optimistic upper limit for the efficiency of grain formation (largely unknown) is  $\sim 40\%$ . Thus,  $f_{in} \leq 0.1$ , but likely to be typically smaller than this value. Given our present ignorance of the processes governing dust formation, we will explore below (see Fig. 7) the effects of varying  $f_{in}$  within a range of reasonable values. For the last two free parameters, which describe the outflow process, i.e.  $w$  and  $\delta$ , the outflow rate (in units of the SFR) and the dust fractional content of the outflow, we take  $0 < w < 90$  and  $0 < \delta < 1$  in order to cover a reasonably large parameter space. Fig. 6 shows the main results of this Section. There we plot the solutions for different values of  $w$  and  $\delta$  and compare them with the data points corresponding to the dust-to-gas vs. metallicity relation shown in Fig. 5. The model results are shown for both a Salpeter (solid lines) and a Scalo (dashed) IMF. Several interesting points can be made from an inspection of this Fig. 6.

First, we conclude that a simple power-law does not represent a good fit to the data, but a more much physically meaningful functional is the one given by eq. 18. For low values of  $\mathcal{D}$  the relation is shown to be quasi-linear, whereas for higher values the shape of the curve depends sensitively on  $\delta$  and  $w$ , through the coefficient  $a$  in eq. 18. In general, for a fixed value of  $\delta$ , a higher value of the outflow rate produces a flatter curve; the same effect can be obtained by decreasing  $\delta$ : both situations allow the system to retain a larger fraction of dust. However, the solutions only depend on the product  $\chi = w(1 - \delta)$ , as can be seen from the coefficient  $a$  in eq. 17;  $\chi$  can be interpreted as a “differential” outflow rate.

Next, we note that the  $\mathcal{D} - X_o$  relation *does not* depend on the particular SFR  $\psi$  of the galaxy: this could be expected since both metal and dust production are strictly connected implying that the relation found is rather general; however, if all the parameters are constant in time, a given galaxy is forced to move along the appropriate curve as it gets metal and dust enriched. The curves are moderately sensitive to the IMF, with the Scalo IMF covering a larger region of the  $\mathcal{D} - X_o$  plane for the given set of parameters.

The results also point out the importance of outflows for dwarf galaxies. The effect of mass loss is particularly evident in the high- $\mathcal{D}$  part of the curves where it results in a flattening; the data require that most of the dwarfs in the sample must have undergone a substantial outflow episode. The segregation of BCDs in the high metallicity, high dust-to-gas ratio region of the plane can be then explained by a higher SFR with respect to dIrrs, which implies a more substantial enrichment in metals and dust. Support to this hypothesis is lent by the fact that BCDs are all consistent with large values ( $> 20$ ) of the differential outflow rate  $\chi$ , since ultimately the SFR determines the rate of SNe powering the wind.

Some uncertainty affects the low- $\mathcal{D}$ , low- $X_o$  part of the curves which is sensitive to the precise value of  $f_{in}$ , as shown by Fig. 7 for the Scalo IMF. In the limit  $X_i \rightarrow 0$ , eq. 18 reduces to  $\mathcal{D}(X_i) \simeq cX_i = f_{in}X_i$ , i.e. the solution scales linearly with  $f_{in}$ , which we have allowed to vary in  $0.003 \leq f_{in} \leq 0.1$ . Thus the precise value of  $f_{in}$  could be possibly constrained by observations of extremely metal poor objects.

## 5. Summary and Conclusions

We have compared the metallicity and the dust-to-gas ratio in a sample of 44 (28 dIrr + 16 BCD) dwarf galaxies. The dust mass has been derived from the FIR emission assuming that the dust composition is the same for all galaxies. We have carried out various tests in order to check the reliability of this dust mass determination. For the sample of dIrr galaxies we found a good correlation between the two quantities, obeying the empirical relation  $12+\log(\text{O}/\text{H}) \propto (0.52 \pm 0.25) \times \log(M_{\text{dust}}/M_{\text{HI}})$ . For BCD galaxies we did not find such a good correlation; both the dust-to-gas ratio and the metallicity tend to be higher than in the dIrr sample, and for a given metallicity the dust-to-gas ratio is on average higher than for the dIrr galaxies.

We have derived a simple analytical form for the expected dust-to-gas ratio vs. metallicity,  $\mathcal{D} - X_o$ , relation (we have assumed that oxygen is a good metallicity indicator) and compared it with the observational data. The main results are the following:

- For low values of  $\mathcal{D}$  the  $\mathcal{D} - X_o$  relation is shown to be quasi-linear, whereas for higher values the curve strongly deviates from the linear behavior.
- The deviation from the linear behavior depends critically on the parameter  $\chi = w(1 - \delta)$ , the “differential” mass outflow rate from the galaxy in units of the SFR  $\psi$ , and is negative if  $\chi < 5$ . Most of the galaxies in the sample can then be inferred to have undergone a substantial outflow episode.
- The *shape* of the  $\mathcal{D} - X_o$  curve does not depend on the SFR,  $\psi$ , of the galaxy but only on the outflow rate; however, the specific location of a given galaxy on the curve does depend on  $\psi$ .
- The BCD metallicity segregation is due to a higher SFR, also suggested by their consistency with the generally larger values of the outflow rates required. The lack of correlation could then be produced by largely different star formation rates and values of  $\chi$  in these objects.

We would like to thank E. Dwek and C. Xu for helpful and interesting discussions and an anonymous referee for useful suggestions. U. L. gratefully acknowledges the receipt of a grant by the Deutsche Forschungsgemeinschaft (DFG) and by the Comisión Interministerial de Ciencia y Tecnología (Spain). This research has made use of the NASA/IPAC extragalactic database (NED) and of the Lyon-Meudon Extragalactic Database (LEDA).

## REFERENCES

- Andreani, P., Casoli, F. & Gerin, M. 1995, *A&A*, 300, 43
- Arnett, D. W. 1990, in *Chemical and Dynamical Evolution of Galaxies*, eds. F. Ferrini et al. (Pisa: ETS), 409
- Borkowski, K. J. & Dwek, E. 1995 *ApJ*, 454 254
- Bouchet, P., Lequeux, J., Maurice, E., Prévot, L.& Prévot-Burnichon, M.L. 1985, *A&A* 149, 330
- Campbell, A., Terlevich, R.& Melnick, J. 1986, *MNRAS*, 223, 811
- Clayton, G.C., Green, J., Wolff, M.J., Zellner, N.E.B., Code, A.D., Davidsen, A.F., et al. 1996, *ApJ*, 460, 313
- Cohen, R.S., Dame, T.M., Garay, G., Montani, J., Rubio, M.& Thaddeus, P. 1988, *ApJ*, 331, L95
- Deharveng, J. M., Sasseen, T. P., Buat, V., Bowyer, S., Lampton, M. & Wu, X. 1994, *A&A*, 289, 715

- Désert, F. X., Boulanger, F. & Puget, J. L. 1990, *A&A*, 237, 215
- de Vaucouleur, G., de Vaucouleur, A., Corwin H., et al. , 1991, *Third Reference Catalog of Galaxies*, (New York: Springer) (RC3)
- Devereux, N. A. & Young, J. S. 1990, *ApJ*, 359, 42
- Donas, J. & Deharveng, J. M. 1984, *A&A*, 140, 325
- Donas, J., Deharveng, J. M., Laget, M., Milliard, B. & Huguenin, D. 1987, *A&A*, 180, 12
- Dwek, E. & Scalo, J. M. 1980, *ApJ*, 239, 193
- Elfhag, T., Booth, R. S., Höglund, B., Johansson, L. E. B. & Sandqvist, Aa. 1996, *A&AS*, 115, 439
- Fanelli, M. N., Waller, W. W., Smith, D. A., Freedman, W. L., Madore, B., Neff, S. G., O'Connell, R. W., Roberts, M. S., Bohlin, R., Smith, A.M. & Stecher, T. P. 1997, *ApJ*, 481, 735
- Ferrara, A., Ferrini, F., Franco, J., & Barsella, B. 1991, *ApJ*, 381, 137
- Fitzpatrick, E.L. 1986, *AJ*, 92, 1068
- Fouqué, P. 1983, *A&A*, 122, 273
- Franco, J. & Cox, D. P. 1986, *PASP*, 98, 1076
- Hildebrand, R. H. 1983, *QJRAS*, 24, 267
- Hill, R. S., Home, A. T., Smith, A. M., Bruhweiler, F. C., Cheng, K. P., Hintzen, P. M. N. & Oliverson, R. J. 1994, *ApJ*, 430, 568
- Huchtmeier, W. K. & Richter O.-G. 1989, *A General Catalogue of HI Observations of Galaxies*, (New York: Springer)
- Huchtmeier, W.K., Hopp, U. & Kuhn, B. 1997, *A&A*, 319, 67
- Hunter, D. A., Gallagher, J. S. & Rautenkranz, D. 1982, *ApJS*, 49, 53
- Hunter, D. A., Gallagher, J. S., Rice W. L., & Gillett, F. C. 1989, *ApJ*, 336, 152
- Hunter, D. A., Hawley, W. N. & Gallagher, J. S. 1993, *AJ*, 106, 1797
- Jones, A. P., Tielens, A. G. G. M., Hollenbach, D. J. & McKee, C. F. 1994, *ApJ*, 433, 797
- IRAS Faint Source Catalog, 1990, Version 2.0, Moshir M. et al. Infrared Processing and Analysis Center
- Issa, M. R., MacLaren, I. & Wolfendale, A. W. 1990, *A&A*, 236, 237
- Kennicutt, R. C. & Kent, S. M. 1983, *AJ*, 88, 1094
- Koornneef, J., 1982 *A&A*, 107, 247
- Kozasa, T, Hasegawa, H. & Nomoto, K. 1989, *ApJ*, 344, 325
- Kunth, D. & Sèvre, F. 1986, in *Star forming dwarf galaxies and related objects*, eds. Kunth, Thuan & Tran-Thanh, (Gif-sur-Yvette: Frontière)
- Larson, R. B. 1996, in *The Interplay between Massive Star Formation, the ISM and Galaxy Evolution*, 11th IAP Meeting, eds. D. Kunth et al. (Gif-sur-Yvette: Frontière), 3
- Lisenfeld, U., Völk, H.J. & Xu, C. 1996, *A&A*, 306, 677
- Maeder, A. 1992, *A&A*, 265, 105
- Masegosa, J., Moles, M. & Campos-Aguilar, A. 1994, *ApJ*, 420, 576
- McGaugh, S. 1991, *ApJ*, 380, 140

- McKee, C. F. 1989, in *Interstellar Dust*, IAU Symp. 135, eds. L. J. Allamandola & A. G. G. M. Tielens, (Dordrecht: Kluwer), 431
- Melisse, J. P. M. & Israel, F. P. 1994a, *A&AS*, 103, 391
- Melisse, J. P. M. & Israel, F. P. 1994b, *A&A*, 285, 51
- Moseley, S. H., Dwek, E., Glaccum, W., Graham, J. R., Loewenstein, R. F. & Silverberg, R. F. 1989, *Nature*, 340, 697
- Norman, C. A. & Ikeuchi, S. 1989, *ApJ*, 345, 372
- Rowan-Robinson, M. 1992, *MNRAS*, 258, 787
- Rubio, M., Garay, G., Montani, J. & Thaddeus, P. 1991, *ApJ*, 368, 173
- Scalo, J. M. 1986, *Fund. Cosm. Phys.*, 11, 1
- Schmidt K. H. & Boller T. 1993, *Astron. Nachr.*, 314, 361
- Skillman, E. D., Kennicutt, R.C. & Hodge, P. W. 1989, *ApJ*, 347, 875
- Sodroski, T.J., Dwek, E., Hauser, M. G. & Kerr, F.J. 1987, *ApJ*, 322, 101
- Staveley-Smith, L., Davies, R.D., Kinman, T.D., 1992, *MNRAS*, 258. 334
- Tavelich, R., Melnick, J., Masegosa, J. & Moles, M. 1992, *A&AS*, 91, 285
- Tinsley, B. M. 1980, *Fund. Cosm. Phys.*, 5, 287
- van den Bergh, S. 1983, *PASP*, 95, 388
- Xu, C. & de Zotti G. 1989, *A&A*, 225, 12
- Xu, C. & Buat, V. 1995, *A&A*, 293, L65
- Xu, C. & Helou, G. 1996, *ApJ*, 456, 163
- Young, J. S., Xie, S., Kenney, J. D. & Rice W. L. 1989, *ApJS*, 261. 492
- Young, J. S., Shuding, X., Tacconi, L., et al. 1995, *ApJS*, 98, 219

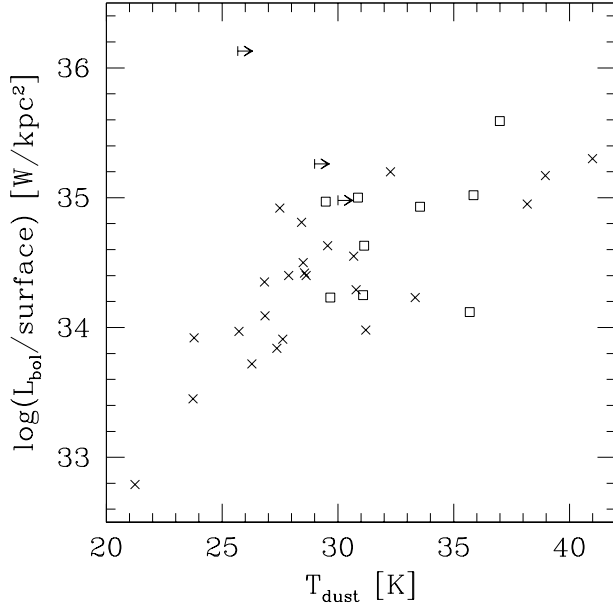


Fig. 1.— Bolometric surface brightness vs. dust temperature for both samples. The open squares denote BCDs with FIR detections, the arrows BCDs with upper limits in the  $100 \mu\text{m}$  flux, and the crosses dIrr galaxies with FIR detections.

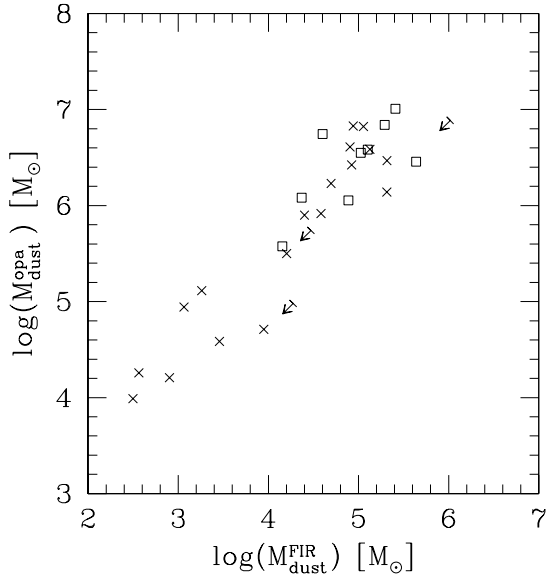


Fig. 2.— Dust masses calculated from the  $60$  and  $100 \mu\text{m}$  fluxes ( $M_{dust}^{FIR}$ ) and from the opacity ( $M_{dust}^{opa}$ ). The symbols are defined as in Fig. 1.

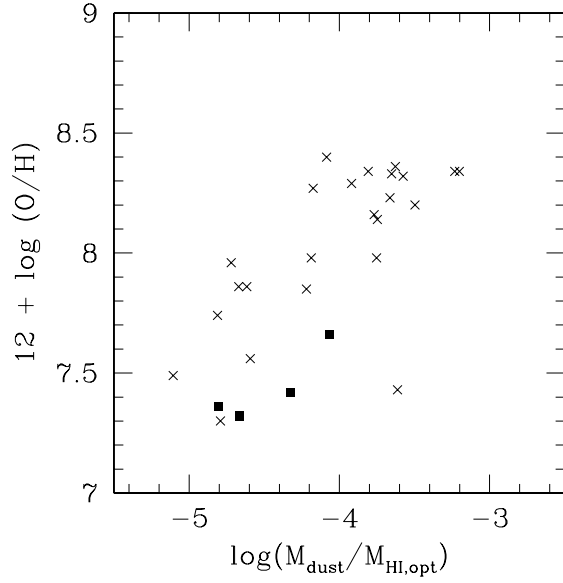


Fig. 3.— Dust-to-gas-ratio and metallicity for the dIrr sample. Filled squares denote galaxies for which  $M_{\text{dust}}$  is undetermined and only an indicative value is plotted (see text).

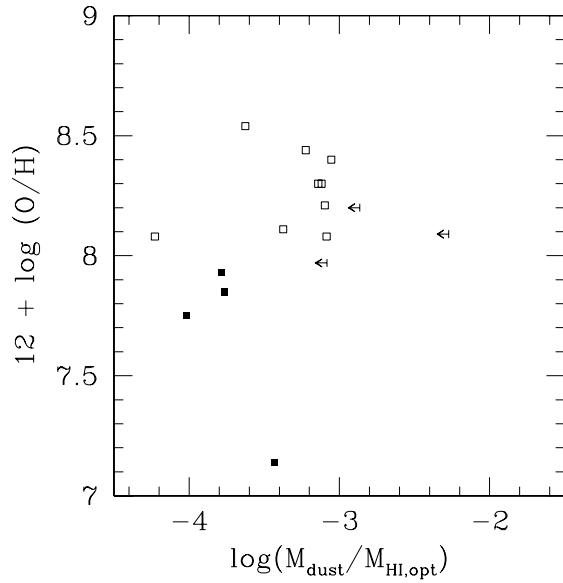


Fig. 4.— Dust-to-gas-ratio and metallicity for the BCD sample. The arrows denote upper limits in the  $100 \mu\text{m}$  flux and filled squares denote galaxies for which  $M_{\text{dust}}$  is undetermined and only an indicative value is plotted (see text).

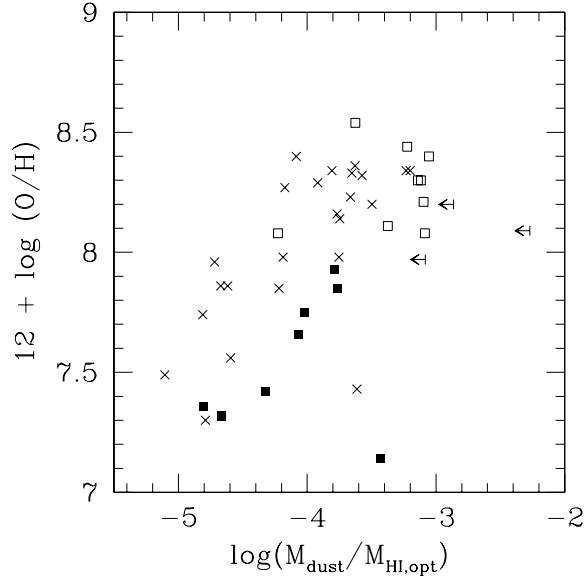


Fig. 5.— Dust-to-gas-ratio and metallicity for both samples (dIrrs and BCDs) together. The symbols are defined as in Fig. 1 and 3

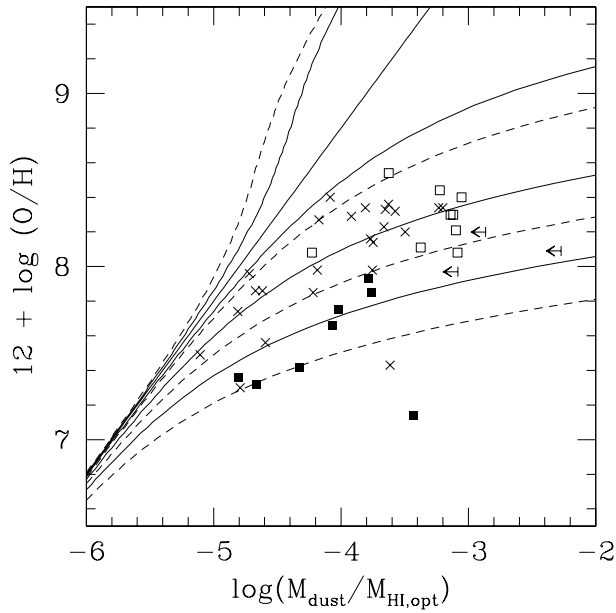


Fig. 6.— Comparison between the theoretical  $\mathcal{D} - X_o$  curves given by eq. 18 and data points for the entire sample (symbols as in Fig. 1 and 3). Solid curves refer to Salpeter IMF, dashed curves refer to Scalo IMF. Each set curves is plotted for  $f_{in} = 0.01$  and the following values of  $\chi = w(1 - \delta) = 0, 5, 10, 30, 90$ , from top to bottom.



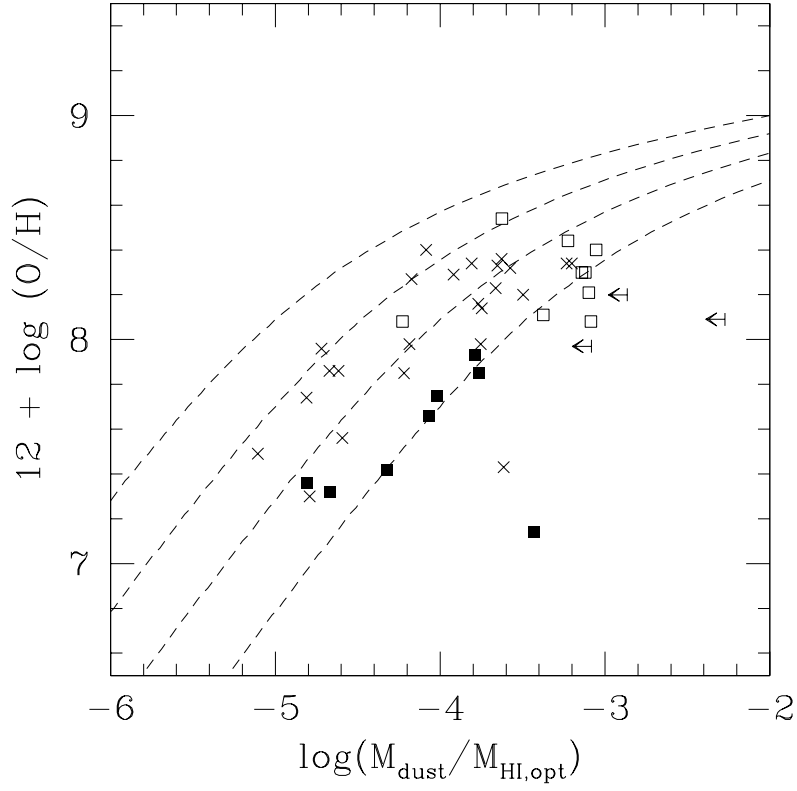


Fig. 7.— Comparison between the theoretical  $\mathcal{D} - X_o$  curves given by eq. 18 and data points for the entire sample (symbols as in Fig. 1 and 3) for different values of  $f_{in} = 0.1, 0.03, 0.01, 0.003$ , from bottom to top, a Scalo IMF and a fixed value of  $\chi = 10$ .

Table 1: Data of the dwarf irregular sample

Name	D [Mpc]	$f_{60}$ [Jy]	$f_{100}$ [Jy]	$\log(M_{\text{dust}})$ [ $M_{\odot}$ ]	$\log(M_{\text{HI,opt}})^{(1)}$ [ $M_{\odot}$ ]	$\log(\frac{M_{\text{dust}}}{M_{\text{HI,opt}}})^{(1)}$	$12 + \log(O/H)$
Gr 8	2.20	0.020	0.143	3.06	6.68	-3.61	7.43
Leo A	1.60	0.090	0.270	2.50	7.29	-4.79	7.30
WLM	1.00	0.320	1.040	2.73	7.54	-4.81	7.74
SMC	0.06	6688.910	15021.930	4.20	8.39	-4.19	7.98
LMC	0.05	82917.000	184686.690	5.13	8.33	-3.20	8.34
DDO 47	2.00	0.125	0.555	3.26	7.48	-4.22	7.85
Sex A	1.50	0.503	0.849	2.56	7.67	-5.11	7.49
Sex B	1.70	0.246	0.684	2.90	7.50	-4.59	7.56
IC 10	2.60	31.230	71.250	5.16	8.66	-3.50	8.20
IC1613	0.70	1.420	3.690	2.82	7.44	-4.62	7.86
IC2574	2.40	2.410	10.620	4.70	8.45	-3.75	7.98
IC4662	2.20	7.360	11.230	3.95	7.87	-3.92	8.29
IC5152	3.00	2.461	6.861	4.40	8.03	-3.63	8.36
NGC55	2.00	77.000	174.100	5.32	8.97	-3.65	8.33
NGC1156	6.50	5.170	9.200	4.91	8.57	-3.66	8.23
NGC1569	2.20	39.223	31.748	3.98	7.75	-3.77	8.16
NGC2366	3.30	3.303	4.578	3.85	8.57	-4.72	7.96
NGC3510	8.90	0.598	1.457	4.58	8.67	-4.08	8.40
NGC4214	4.10	14.470	25.470	4.94	8.75	-3.81	8.34
NGC4236	4.90	3.980	10.020	4.92	9.10	-4.17	8.27
NGC4449	3.90	14.762	37.806	5.31	8.89	-3.57	8.32
NGC5253	6.90	30.510	29.360	5.06	8.29	-3.23	8.34
NGC5408	4.20	2.360	2.160	3.46	8.13	-4.67	7.86
NGC6822	0.50	47.630	95.420	3.77	7.52	-3.75	8.14
SDIG	2.90	< 0.093	< 0.159	2.42	6.74	-4.32	7.42
UGC4483	4.00	< 0.079	< 0.149	2.73	7.40	-4.67	7.32
DDO 167	3.50	< 0.093	< 0.183	2.73	6.80	-4.07	7.66
DDO 187	2.60	< 0.084	< 0.134	2.20	7.01	-4.81	7.36

<sup>(1)</sup>  $M_{\text{HI,opt}} = M_{\text{HI}}/2$  refers to the HI mass inside the optical diameter (see text)

Table 2: Data of the Blue Compact Dwarf sample

Name	D	$f_{60}$	$f_{100}$	$\log(M_{\text{dust}})$	$\log(M_{\text{HI,opt}})^{(1)}$	$\log(\frac{M_{\text{dust}}}{M_{\text{HI,opt}}})^{(1)}$	$12 + \log(O/H)$
	[Mpc]	[Jy]	[Jy]	$[M_{\odot}]$	$[M_{\odot}]$		
UM 448	6.00	4.140	4.321	4.16	7.24	-3.09	8.08
IC 3258	21.20	0.490	0.970	5.03	8.25	-3.22	8.44
Mrk 7	42.30	0.480	0.970	5.64	9.26	-3.63	8.54
Mrk 33	21.60	4.680	5.300	5.41	8.47	-3.05	8.40
Mrk 35	14.50	4.950	6.740	5.29	8.43	-3.14	8.30
Mrk 450	12.10	0.480	0.820	4.37	7.47	-3.10	8.21
NGC4670	12.10	2.630	4.470	5.10	8.22	-3.12	8.30
NGC4861	12.90	1.970	2.260	4.60	8.83	-4.23	8.08
II Zw70	17.60	0.710	1.240	4.89	8.26	-3.37	8.11
UM 455	51.10	– <sup>(2)</sup>	– <sup>(2)</sup>	5.59	9.61	-4.02	7.75
Mrk 600	14.00	– <sup>(2)</sup>	– <sup>(2)</sup>	4.46	8.23	-3.76	7.85
IZw 18	11.00	– <sup>(2)</sup>	– <sup>(2)</sup>	4.25	7.68	-3.43	7.14
IZw 36	4.80	– <sup>(2)</sup>	– <sup>(2)</sup>	3.53	7.32	-3.79	7.93
IIZW40	10.10	6.020	<19.700	6.02	8.29	-2.27	8.09
Mrk750	12.40	0.440	<0.840	4.47	7.34	-2.86	8.20
IZw123	10.40	0.300	<0.640	4.28	7.36	-3.08	7.97

<sup>(1)</sup>  $M_{\text{HI,opt}} = M_{\text{HI}}/2$  refers to the HI mass inside the optical diameter (see text)

<sup>(2)</sup> not detected by IRAS